The EMBO Journal Vol. 20 No. 13 pp. 3389–3401, 2001

Fission yeast ch-TOG/XMAP215 homologue Alp14 connects mitotic spindles with the kinetochore and is a component of the Mad2-dependent spindle checkpoint

Miguel Angel Garcia, Leah Vardy, Nirada Koonrugsa and Takashi Toda[1]

Laboratory of Cell Regulation, Imperial Cancer Research Fund, PO Box 123, 44 Lincoln's Inn Fields, London WC2A 3PX, UK

[1]Corresponding author
e-mail: toda@icrf.icnet.uk

The TOG/XMAP215-related proteins play a role in microtubule dynamics at its plus end. Fission yeast Alp14, a newly identified TOG/XMAP215 family protein, is essential for proper chromosome segregation in concert with a second homologue Dis1. We show that the *alp14* mutant fails to progress towards normal bipolar spindle formation. Intriguingly, Alp14 itself is a component of the Mad2-dependent spindle checkpoint cascade, as upon addition of microtubule-destabilizing drugs the *alp14* mutant is incapable of maintaining high H1 kinase activity, which results in securin destruction and premature chromosome separation. Live imaging of Alp14–green fluorescent protein shows that during mitosis, Alp14 is associated with the peripheral region of the kinetochores as well as with the spindle poles. This is supported by ChIP (chromatin immunoprecipitation) and overlapping localization with the kinetochore marker Mis6. An intact spindle is required for Alp14 localization to the kinetochore periphery, but not to the poles. These results indicate that the TOG/XMAP215 family may play a central role as a bridge between the kinetochores and the plus end of pole to chromosome microtubules.

Keywords: fission yeast/kinetochore/spindle checkpoint/TOG/XMAP215

Introduction

The TOG/XMAP215-related proteins constitute a conserved family. XMAP215 was purified originally as a then novel microtubule-associated protein (Gard and Kirschner, 1987). The human homologue ch-TOG was identified independently as cDNA, which was over-expressed in colonic and hepatic tumour cell lines (Charrasse *et al*., 1995, 1998). Mutations in the TOG/XMAP215 homologues were also identified in genetically amenable systems such as yeast, *Drosophila melanogaster* and *Caenorhabditis elegans* (Ohkura *et al*., 1988; Nabeshima *et al*., 1995; Wang and Huffaker, 1997; X.P.Chen *et al*., 1998; Matthews *et al*., 1998; Cullen *et al*., 1999). Biochemical and cell biological analysis in vertebrates has suggested that the TOG/XMAP215 protein plays a positive role in microtubule stability, in particular by stimulating the growth rate at the plus end (Gard and Kirschner, 1987; Vasquez *et al*., 1994; Tournebize *et al*., 2000). Genetic analysis from yeast, worm and fly has shown that this family is important for spindle formation, and localizes to the spindle poles (Nabeshima *et al*., 1995; Nakaseko *et al*., 1996; Wang and Huffaker, 1997; X.P.Chen *et al*., 1998; Matthews *et al*., 1998; Wigge *et al*., 1998; Cullen *et al*., 1999).

Pole to chromosome microtubules play a central role in proper chromosome segregation at anaphase. Whilst the minus ends of these microtubules originate from the spindle poles, the plus end specifically interacts with and is embedded in the kinetochore, the specialized structure on centromeric DNA. Pairs of the sister chromatids have to be kept together until pole to chromosome microtubules capture all the unattached kinetochores in a bivalent fashion, otherwise precocious separation of sister chromatids results in aneuploid offspring, which leads to cell death or tumorigenesis (Lengauer *et al*., 1998). In order to prevent such a deleterious consequence, the cell has developed a regulatory system, called the spindle assembly checkpoint. The molecular network of this pathway has been revealed by genetic approaches in budding yeast (Hoyt *et al*., 1991; Li and Murray, 1991; Weiss and Winey, 1996), and subsequent work shows that this surveillance mechanism is conserved ubiquitously (Li and Benezra, 1996; Taylor and McKeon, 1997; Cahill *et al*., 1998; Jin *et al*., 1998; Taylor *et al*., 1998).

The major, though not only, pathway of the spindle assembly checkpoint is the kinetochore-mediated network, which is composed of Mad1, 2 and 3, and Bub1 and 3 (Hoyt *et al*., 1991; Li and Murray, 1991). These proteins localize to the unattached kinetochores during mitosis in vertebrates (R.-H.Chen *et al*., 1996, 1998; Li and Benezra, 1996; Taylor and McKeon, 1997; Taylor *et al*., 1998; Waters *et al*., 1998). As the cell monitors the physical state of, or tension at, kinetochores, these checkpoint proteins bind in concert to the Slp1/Cdc20/Fizzy protein, a positive regulator of the APC/C ubiquitin ligase (anaphase-promoting complex/cyclosome) (King *et al*., 1995; Sudakin *et al*., 1995), thereby inhibiting its activation (Hwang *et al*., 1998; Kim *et al*., 1998). Two major substrates for the APC/C are mitotic cyclins and securins, the destruction of which is required for exit from mitosis and sister chromatid segregation, respectively (King *et al*., 1996). The central question that remains to be answered is how unattached or tensionless kinetochores are recognized and their information transduced to the Mad2-dependent checkpoint machinery. Also, the mechanism of how the plus end of spindle microtubules interacts with the kinetochores is a crucial issue that needs to be addressed.

Fission yeast *alp*$^+$ genes have been identified as loci that are required for the maintenance of growth polarity control (*alp1–15* loci, altered polarity) (Radcliffe *et al*., 1998). In line with the fact that the microtubule cytoskeleton is a crucial determinant of growth polarity in this yeast, many

of the *alp*$^+$ genes encode conserved proteins that are required for microtubule and spindle function (Hirata *et al*., 1998; Radcliffe *et al*., 1999; Vardy and Toda, 2000). Here we show that fission yeast Alp14, a member of the conserved TOG/XMAP215 proteins, plays an essential role as a connection between the kinetochores and pole to chromosome microtubules.

Results

Alp14 is required for bipolar spindle formation and proper chromosome segregation

In addition to growth polarity defects, temperature-sensitive (ts) *alp14-1270* mutants displayed abnormal mitotic spindles and mis-segregated chromosomes when incubated at 36°C (Figure 1A). In order to characterize the ts *alp14* phenotypes in more detail, a synchronous culture was prepared by centrifugal elutriation using an *alp14-1270* strain containing the integrated *cut12*$^+$*-GFP* gene (*cut12*$^+$ encodes an integral component of the spindle pole body, SPB; *GFP* encodes green fluorescent protein) (Bridge *et al*., 1998), and microtubules and the SPB were observed with confocal microscopy. Synchrony was followed in the culture incubated at 26°C (Figure 1B).

At the restrictive temperature, the first phenotype observed was short and misorientated interphase microtubules (20 min, the second panels in Figure 1C). Note that at 0 min at 26°C, the length and structure of these microtubules were normal (top panels). Then upon entry into mitosis, three types of defects in mitotic spindles appeared sequentially. At 120 min when cells entered mitosis, dense and thick dots of microtubules were observed (24%, shown by arrows), which are never seen in wild-type cells. The SPB had not separated in these cells. Then mitotic cells with monopolar spindles (asterisk) were observed. It appeared that *alp14* mutants failed to progress towards bipolar spindle formation. Despite the lack of normal bipolar spindles, anaphase and post-anaphase cells then appeared (arrowheads). It is particularly noticeable that in these cells, long anaphase spindles were rarely observed; instead, discontinuous or misorientated spindles/microtubules, some of which were associated with the SPBs, remained. This result suggested that Alp14 is required for the formation of both interphase microtubules and bipolar mitotic spindles, and plays a role in the completion of exit from anaphase at 36°C.

Fission yeast contains two TOG-related genes, alp14$^+$ *and dis1*$^+$*, which play an overlapping role*

We cloned the *alp14*$^+$ gene by complementation from a fission yeast genomic library. Nucleotide sequencing showed that the *alp14*$^+$ gene encodes a protein that belongs to a family of conserved microtubule-binding proteins, including vertebrate ch-TOG (Charrasse *et al*., 1995, 1998), *Xenopus* XMAP215 (Gard and Kirschner, 1987), *Drosophila* mini spindles (Msps) (Cullen *et al*., 1999), *C.elegans* ZYG-9 (Matthews *et al*., 1998), budding yeast Stu2 (Wang and Huffaker, 1997) and fission yeast Dis1 (Nabeshima *et al*., 1995) (Figure 2A and B). The TOG/XMAP215 family contains the N-terminal repeated domains. Recently it has been shown that the conserved TOG domains comprise HEAT repeats (Andrade and Bork, 1995; Neuwald and Hirano, 2000), the hallmark of protein–protein interaction motifs (Groves *et al*., 1999). Proteins containing HEAT repeats include XCAP-D2 and XCAP-G (condensin), Scc2 (cohesin), COP-1 (coatomer) and PR65/A (type IIA protein phosphatase). Indeed, the TOG domains of Alp14 also consist of HEAT repeats (Figure 2A).

Gene disruption showed that the *alp14*$^+$ gene is not essential for cell viability. However, *alp14*-deleted cells showed ts phenotypes similar to *alp14-1270* cells (Figure 2C), and defective phenotypes between Δ*alp14* and *alp14-1270* cells were indistinguishable. Given the high degree of homology between Alp14 and Dis1, functional redundancy of these two genes was determined. It turned out that multicopy plasmids containing either gene were capable of rescuing the defects of mutations in the other gene, although suppression of Δ*dis1* by the *alp14*$^+$ gene appeared incomplete (Figure 2C). Furthermore, double mutants between *dis1* and *alp14* were inviable at 30°C, the temperature permissive for both single mutants (Table I). Like ts *stu2* mutants (Wang and Huffaker, 1997), *alp14* mutants displayed strong genetic interactions with mutations in tubulin genes or alterations in tubulin gene expression (Table I). Therefore, Alp14 and Dis1 are functional, as well as structural, homologues, and Alp14 plays a major role in cells grown at high temperature (36°C), whilst Dis1 is required for growth at low temperature (18°C).

alp14 mutants activate the Mad2-dependent spindle assembly checkpoint transiently at the restrictive temperature

Given the appearance of abnormally segregated chromosomes and defective spindles in the *alp14* mutant, whether or not the spindle assembly checkpoint pathway was activated was addressed. To this end, at first, a double mutant between the *mad2* deletion and *alp14-1270* was constructed, and defective phenotypes at the restrictive temperature were examined. As shown in Figure 3A, a Δ*mad2alp14-1270* double mutant lost viability rapidly (triangles) at 36°C, compared with the single *alp14-1270* mutant (circles). Phenotypic analysis showed that the double mutant, but not the single, displayed 'cut' phenotypes, the combination of a chromosome attachment failure with a spindle checkpoint defect (Figure 3B). Albeit viable at 26°C, *alp14-1270* mutants, as well as Δ*alp14*, have defects in chromosome stability as, using the standard mini-chromosome assay (Niwa *et al*., 1989), we failed to obtain any Ade$^+$ colonies, suggesting that mini-chromosomes are extremely unstable in this mutant.

In vertebrates, when the spindle checkpoint is activated, Mad2 localizes to unattached kinetochores (R.-H.Chen *et al*., 1996, 1998; Li and Benezra, 1996; Taylor and McKeon, 1997; Taylor *et al*., 1998; Waters *et al*., 1998). As Mad2 localization has not been reported in fission yeast, its similarities to mammalian cells were examined. In cold-sensitive *nda3-311* mutants, which are defective in β-tubulin (Hiraoka *et al*., 1984) and activate the checkpoint, the chromosomal *mad2*$^+$ gene was tagged with green fluorescent protein (GFP) at the C-terminus. It was concentrated on a single dot, or sometimes three dots, on condensed chromosomes (Figure 3C). It was also found that Mad2 was concentrated to a nuclear dot when the spindle checkpoint was activated in wild-type cells by

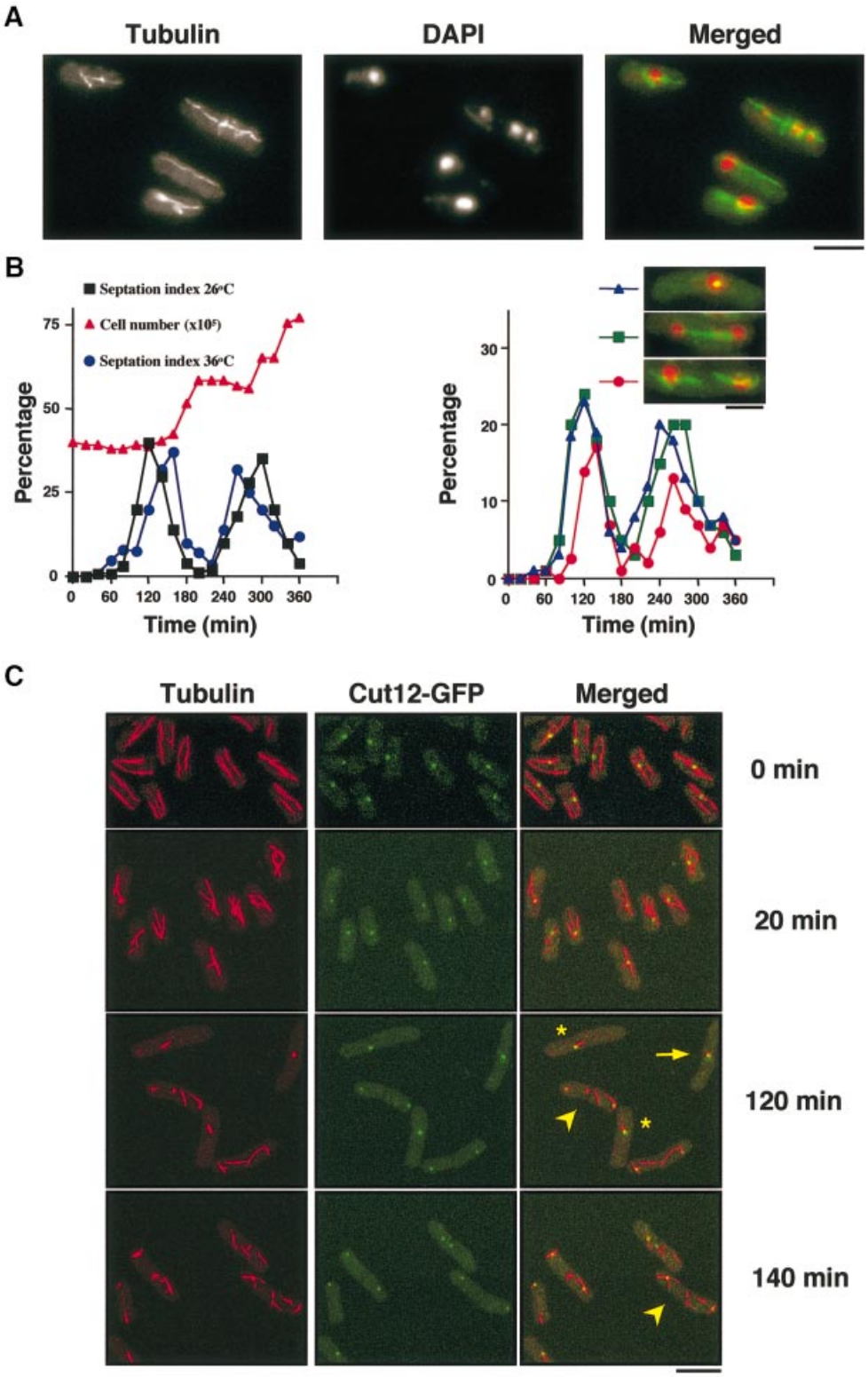

Fig. 1. Alp14 is required for bipolar spindle formation. (**A**) Microtubule structures and nuclear staining in *alp14-1270* mutants. Exponentially growing *alp14-1270* mutants at 26°C were shifted up to 36°C, incubated for 6 h and processed for immunofluorescence microscopy. (**B**) Synchronous culture analysis. Small early G_2 cells of *alp14-1270* mutants were collected by centrifugal elutriation and the cultures were divided into two parts, one part incubated at 26°C and the other shifted to 36°C. Septation index (left panel, black squares at 26°C and blue circles at 36°C) and cell number (left, at 26°C, red triangles) were plotted. Note that the peak of septation was shifted 40 min afterward at 36°C, compared with 26°C (160 min versus 120 min). The percentage of cells containing dense short spindles (right panel, blue triangles, shown in inset and arrows in C), cells with separated SPBs and continuous spindles (green squares), and cells with abnormal anaphase spindles (red circles, shown in inset and arrowheads in C) is shown on the right. (**C**) Abnormal microtubules and spindles in *alp14* mutants. Representative images from synchronous culture analysis at 0, 20, 120 or 140 min are shown (anti-tubulin, Cut12–GFP and merged images). Cells that have dense short spindles (arrows), monopolar spindles (asterisks) and misorientated anaphase spindles (arrowheads) are marked. The bar indicates 10 μm.

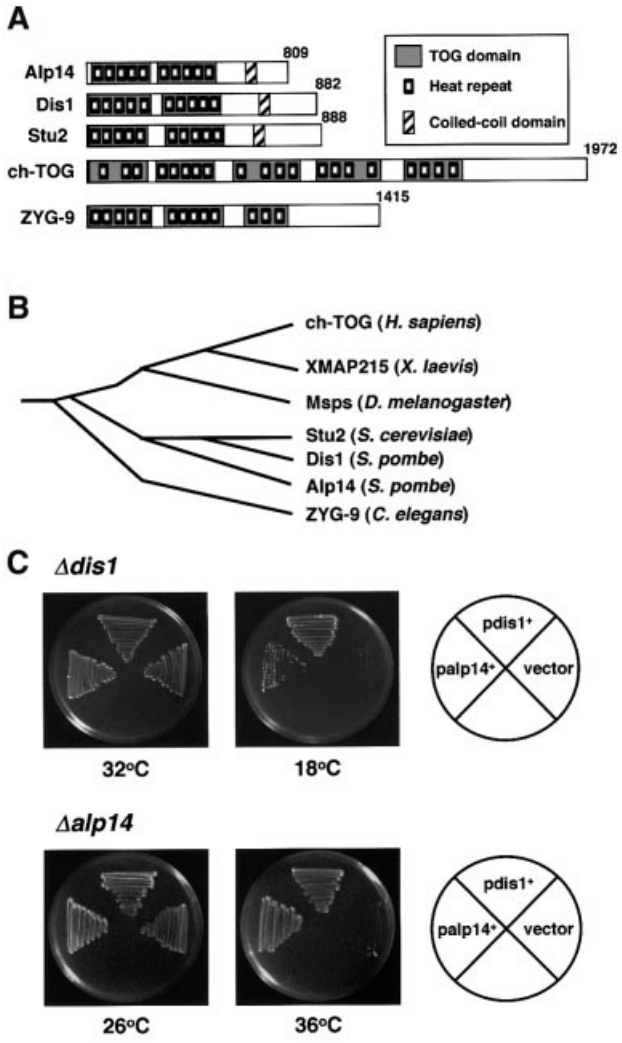

Fig. 2. Structural comparison between Alp14 and TOG-related proteins. (**A**) 'TOG' domains (dark boxes), HEAT-repeating units (small boxes) (Neuwald and Hirano, 2000) and coiled-coil regions (hatched) are shown in different members of the TOG/XMAP215 family from various organisms. These include Alp14, Dis1 (*Schizosaccharomyces pombe*), Stu2 (*Saccharomyces cerevisiae*), ch-TOG (*Homo sapiens*) and ZYG-9 (*Caenorhabditis elegans*). (**B**) Phylogenetic trees. ClustaIX dendrogram of the relationship between human, frog (XMAP215), fly (Msps), worm, budding and fission yeast proteins is shown. (**C**) Functional exchangeability between Alp14 and Dis1. Δ*dis1* (upper) or Δ*alp14* mutants (lower) containing an empty vector, and multicopy plasmids carrying *dis1*$^+$ or *alp14*$^+$ were streaked at either 18 (upper middle), 26 (lower left), 32 (upper left) or 36°C (lower middle) and incubated for 3–6 days.

adding the microtubule-destabilizing drug thibendazole (TBZ; Figure 3D, right), whilst in interphase cells (exponentially growing wild-type cells or *alp14* mutants at the permissive temperature), it localizes mostly to the entire nucleus in a discontinuous patched pattern (see Figure 3D, left, and E, left). This localization pattern suggested that, like higher eukaryotes, fission yeast Mad2 localizes to the unattached kinetochores when the spindle checkpoint is activated.

Having established Mad2 localization upon checkpoint activation, its localization in *alp14* mutants at 36°C was examined. When *alp14* mutant cells were arrested with hydroxyurea (HU) at early S phase and released in the absence of HU at 36°C synchronously, Mad2–GFP was found to localize specifically to a spot in abnormal mitotic cells which showed dense and thick dots of microtubules (Figure 3E, middle panels). In normally dividing cells at 26°C, Mad2 localized to the nucleus (left). Despite this specific localization, consistent with cell cycle progression at 36°C shown before (Figure 1B and C), Mad2 was subsequently delocalized and dispersed in the divided nuclei at anaphase (Figure 3E, right panels). Although the cell cycle proceeded, checkpoint activation did result in a delay in cell division, which was evident in the percentage of septated cells in the elutriated culture (see left panel in Figure 1B). Under these conditions, the frequency of septated cells peaked 40 min later than those at the permissive temperature (120 min at 26°C versus 160 min at 36°C).

In order to examine the requirement for Mad2 for the division delay in *alp14* mutants, a similar synchronous

Table I. Genetic interaction between *alp14* and tubulin mutants

Strains	Δ*dis1*	*nda3-311*[a]	*atb2::LEU2*[a]	*nmt1-GFP-atb2*$^+$[b]	*nmt81-GFP-atb2*$^+$[b]
alp14-1270	lethal	lethal	lethal	lethal[c]	toxic[d]

[a]*nda3*$^+$ and *atb2*$^+$ encode β-tubulin and α2-tubulin, respectively.
[b]A thiamine-repressible strong (*nmt1*) or crippled promoter (*nmt81*) was integrated in front of the initiator methionine of the chromosomal *atb2*$^+$ gene.
[c]Strains failed to grow at 26°C not only under derepressed conditions (without thiamine), but also under repressed conditions (in its presence).
[d]In the absence of thiamine (derepressed), strains managed to form colonies, but showed slow growth (150% of doubling time) and defects in cell shape.

Fig. 3. *alp14* mutants transiently activate the Mad2-dependent spindle assembly checkpoint at the restrictive temperature. (**A**) Dependence of viability on Mad2. *alp14-1270* (circles), *mad2*-deleted (crosses) or *mad2alp14-1270* mutants (triangles) were grown at 26°C and shifted up to 36°C. Cell cultures were spread on rich plates after appropriate dilution and incubated at 26°C. At the same time, cell number was counted, and viability (number of viable cells per total number of cells) was calculated. (**B**) Nuclear staining. Cells were stained with 4′,6-diamidino-2-phenylindole (DAPI) after 6 h at 36°C. Note that chromosomes were condensed in *alp14-1270* cells (middle), whilst in *mad2alp14-1270* double mutants (bottom), decondensed chromosomes are evident. (**C**) Localization of Mad2 in tubulin mutants. *nda3-311* mutants containing chromosomally tagged *mad2*$^+$*-GFP* were incubated for 10 h at 20°C. (**D**) Localization of Mad2 upon depolymerization of microtubules. Wild-type cells containing chromosomally tagged *mad2*$^+$*-GFP* were treated with TBZ (50 μg/ml) and incubated for 90 min. Localization of Mad2–GFP was examined before (–TBZ) and after incubation (+TBZ). (**E**) Mad2 localization in *alp14* mutants at 36°C. *alp14* mutant cells containing chromosomally tagged *mad2*$^+$*-GFP* were synchronized with HU at 26°C, washed and released to HU-free medium at 36°C. Signals from Mad2–GFP were observed after 60 and 90 min. Anti-tubulin staining was also performed. The bar indicates 10 μm. (**F**) Mad2-dependent division delay in *alp14* mutants. Wild-type (black squares), *alp14* (green circles) and *alp14*Δ*mad2* mutant cells (red triangles) were synchronized as in (E). The percentage of septated cells was counted every 15 min.

culture experiment was repeated in wild-type, *alp14* and *alp14Δmad2* mutants. As shown in Figure 3F, septation took place earlier in *alp14Δmad2* double mutants (peaked at 105 min) than in a single *alp14* mutant (120 min), indicating that the mitotic delay is attributed to activation of the Mad2 checkpoint. However it should be noted that the timing of septation was not completely reverted in this double mutant, compared with wild-type cells (90 min). This suggested that there is an additional Mad2-independent mechanism, which leads to the division delay in *alp14* mutants. Taken together, these results indicated that the absence of Alp14 results in spindle damage, which

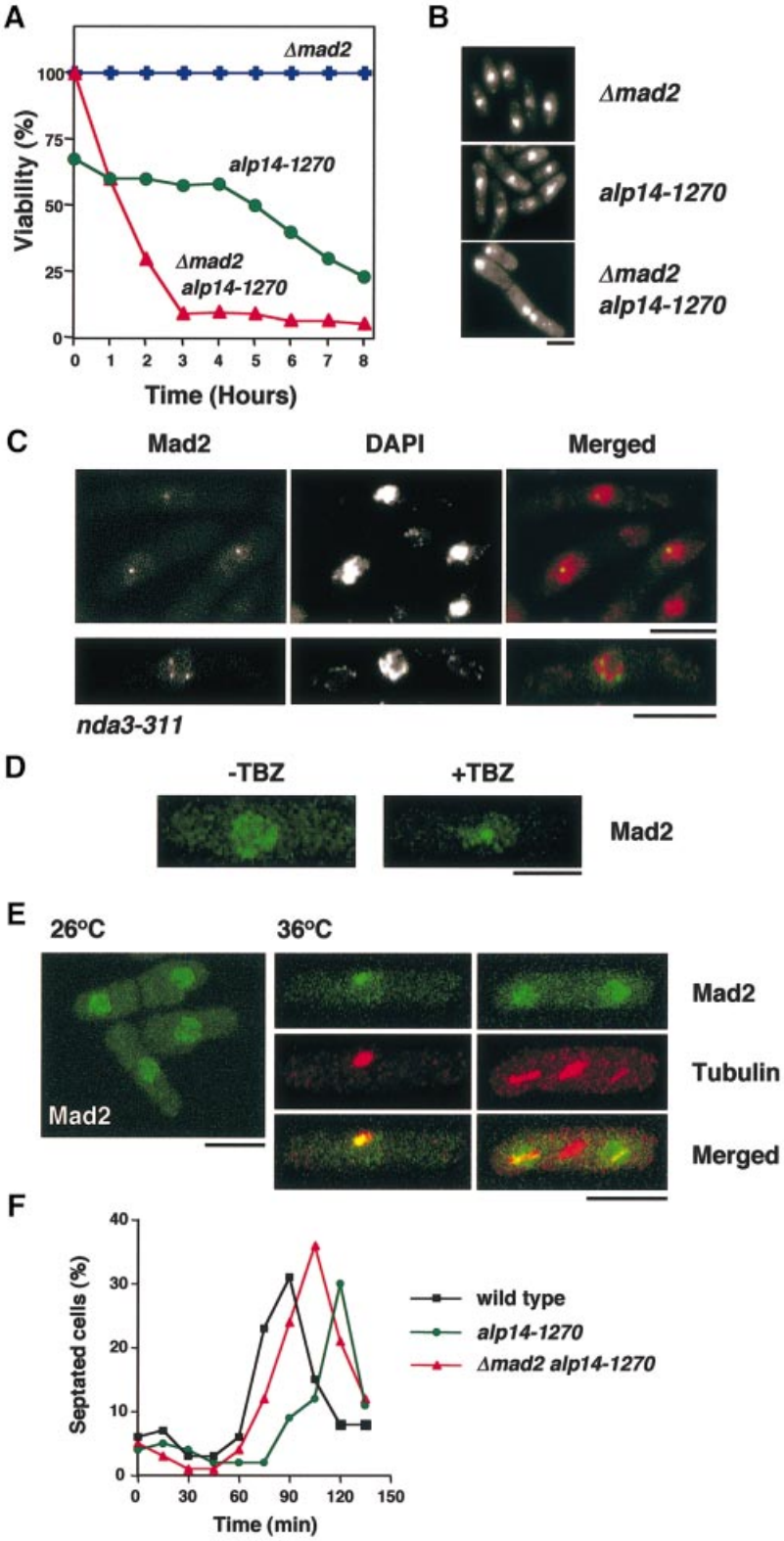

activates the Mad2 checkpoint pathway, leading to division delay; however, this activation was only transient and cell cycle progression continued.

Alp14 is a novel component of the spindle assembly checkpoint and functions in a linear manner upstream of Mad2

Mutants defective in microtubule and/or spindle function often show hypersensitivity to microtubule-destabilizing drugs. We found that the *alp14* mutant was hypersensitive to TBZ even at the permissive temperature (Figure 4A, lanes 4 and 5). This hypersensitivity was rescued by the introduction of plasmids containing either the *alp14*$^+$ or the *dis1*$^+$ gene (lanes 6–8). Cell morphology showed that, surprisingly, *alp14* mutants in the presence of TBZ displayed a cut phenotype (20% after 6 h at 26°C, Figure 4B), rather than a mitotic arrest. In line with this, unlike wild-type cells, viability fell sharply upon TBZ addition (Figure 4C). This suggested that *alp14* mutant cells are defective in the spindle checkpoint.

It is known that mutants defective in the spindle checkpoint pathway fail to maintain H1 kinase activity to high levels under conditions of checkpoint activation (Li and Murray, 1991; He *et al*., 1997). We next sought to examine whether Alp14 function is required for the maintenance of high H1 kinase in the presence of TBZ. Wild-type and *alp14* mutant cells were synchronized with HU, released in the presence of TBZ upon washout of HU, and H1 kinase activity was measured. The H1 kinase activity increased (3 h) and remained at high levels in wild-type cells, whereas *alp14* mutants failed to maintain high activity and declined to low levels (Figure 4D and E).

Another phenotype of spindle checkpoint mutants is premature separation of sister chromatids, which is attributed to the untimely degradation of securin (Cut2 in fission yeast) (King *et al*., 1996). In order to examine securin levels in the *alp14* mutant, immunoblotting using strains containing C-terminally tagged Cut2 (Cut2-HA) (Funabiki *et al*., 1996) was performed. As shown in Figure 4F and G, unlike wild-type cells, Cut2 levels were reduced in *alp14* mutants in the presence of TBZ. Consistent with this result, sister chromatids segregated abnormally in *alp14* mutants, which was visualized using centromere marking GFP–LacI (Cen–GFP) (Straight *et al*., 1996; Nabeshima *et al*., 1998) (Figure 4H), and Mad2 failed to accumulate at the kinetochores (data not shown). These results demonstrate that Alp14 is required for the activation of the spindle checkpoint pathway in the presence of TBZ and strongly suggest that Alp14 is a component of this pathway.

In order to examine a functional relationship between Alp14 and Mad2, cell viability of the *mad2alp14-1270* mutant in the presence of TBZ was compared with each single mutant. It was found that the kinetics of viability loss were indistinguishable between each single and double mutant (Figure 4C). This result showed that Alp14 functions in a linear manner with Mad2. Ectopic overexpression of *mad2*$^+$ activates the checkpoint without spindle damage and arrests the cells in metaphase (He *et al*., 1997; Kim *et al*., 1998). We next asked whether Mad2 overproduction is still capable of activating the checkpoint in *alp14* mutants. As shown in Figure 4I, overexpression of *mad2*$^+$ was still toxic and arrested *alp14* cells in mitosis (data not shown). Overexpression of *alp14*$^+$, on the other hand, cannot be used for this type of analysis, as it disrupts mitotic spindles and activates the checkpoint (data not shown). Taken together, these results show that Alp14 functions either upstream of or in concert with the Mad2 checkpoint protein.

Alp14 localizes to the spindle poles and to dots along mitotic spindles

In order to examine the cellular localization of Alp14, the *GFP* gene was fused to the C-terminus of the chromosomal *alp14*$^+$ gene. GFP tagging did not interfere with protein function as strains containing Alp14–GFP grew as well as wild-type strains at 36°C. GFP signals were examined in fixed samples from exponentially growing wild-type cells. Results are shown in Figure 5, and summarized below. During interphase, Alp14 localized along cytoplasmic microtubules (Figure 5A, arrows) as discontinuous patches, rather than as filamentous structures. Upon entry into mitosis, mitotic spindles were stained (Figure 5B). In addition, the two distal dots, likely to be the SPB, were stained. Upon exit from mitosis, Alp14–GFP appeared to dissociate from long anaphase spindles, and instead co-localized with astral microtubules (Figure 5B, bottom panels, see below). During post-anaphase, Alp14 relocalized to microtubules at the central ring (Figure 5A, arrowhead).

To delineate further the cellular localization of Alp14 during the cell cycle in detail, particularly focusing on mitotic behaviour, time-lapse live imaging of Alp14–GFP was performed using a conventional and confocal laser scanning microscope. As shown in Figure 6A, during phase 2, in which spindle length remains constant (Nabeshima *et al*., 1998), Alp14–GFP localized to four or five intranuclear dots along spindles (2 s intervals). Upon elongation of the spindle (Figure 6B, 75 s and later, phase 3, also see Supplementary data available at *The EMBO Journal* Online), these dots appeared to be pulled polewards and could hardly be localized to the equator of the anaphase spindle. This dynamic movement is very similar to that of centromeric DNAs reported previously (Nabeshima *et al*., 1998). In late anaphase, Alp14 localizes to astral microtubules (arrows in Figure 6C). This analysis establishes the dynamic nature of Alp14 localization along spindles during mitotic phase 2 and phase 3, and suggests that Alp14 localizes to the kinetochores.

Alp14 localizes to the kinetochore periphery during metaphase in a microtubule-dependent manner

Given the involvement of Alp14 in the Mad2-mediated checkpoint pathway and the localization of Alp14 to the intranuclear dots along mitotic spindles, we were interested in whether Alp14 localizes to the kinetochores. To address this question, the following approaches were undertaken. First, Alp14–GFP localization was examined in two mitotically arresting mutants. A *nuc2-663* strain defective in the homologue of Cdc27/Apc3 displays a uniform metaphase arrest at 36°C (Hirano *et al*., 1988), whilst the *nda3-311* mutant arrests at prophase at 20°C (Hiraoka *et al*., 1984). In *nuc2*-arrested cells, Alp14–GFP showed, in addition to the two distal SPBs, three intranuclear dots (Figure 7A, upper) similar to those

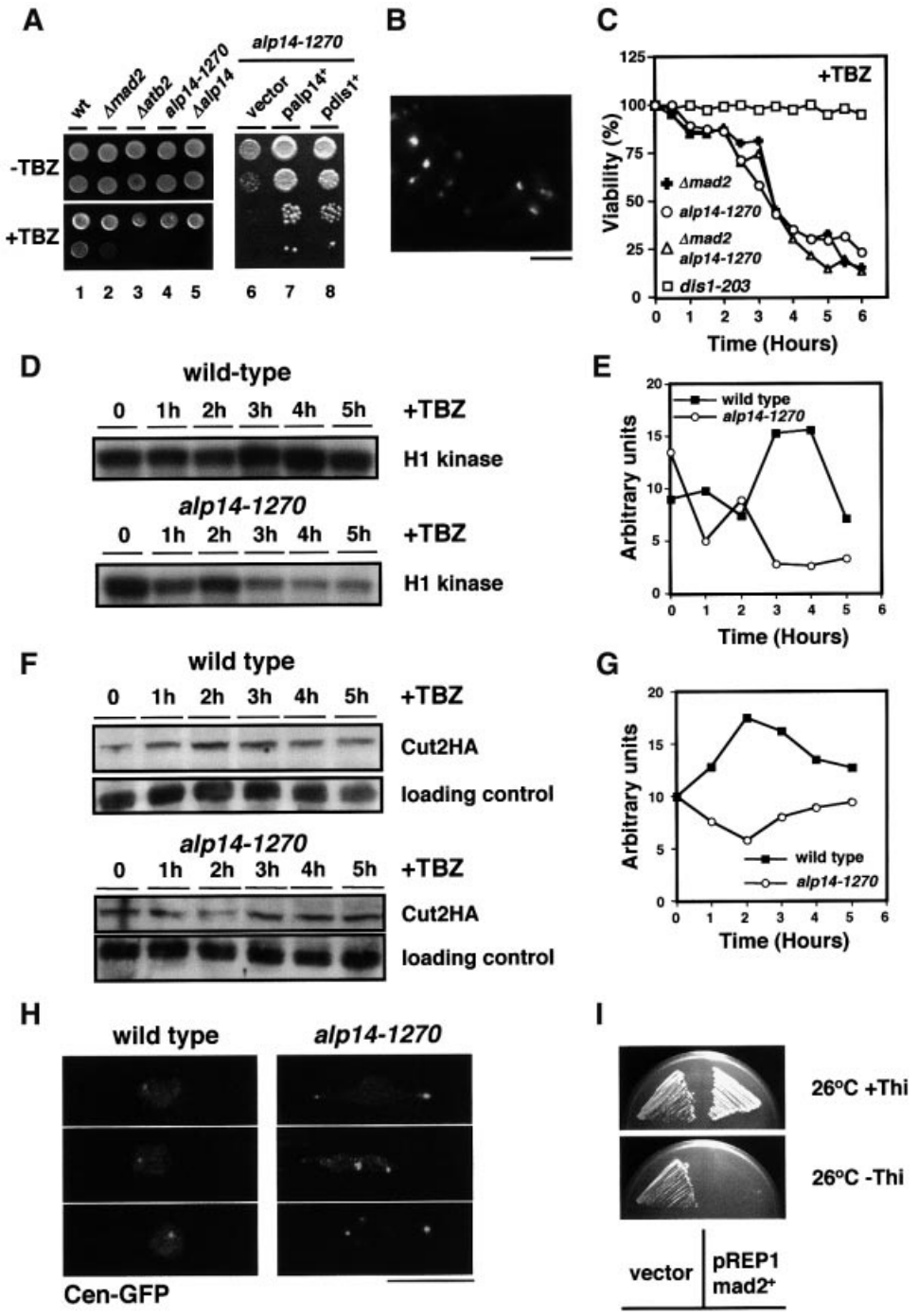

Fig. 4. Alp14 is a component of the Mad2-dependent spindle checkpoint pathway. (**A**) Hypersensitivity to TBZ. Wild-type (lane 1), *mad2*-deleted (lane 2), *atb2*-deleted (lane 3), *alp14-1270* (lane 4) or *alp14*-deleted cells (lane 5) were spotted (10^5 and 10^4 cells) on rich plates in the absence (upper) or presence of 30 μg/ml TBZ for 5 days and incubated at 26°C. Also, *alp14-1270* cells containing an empty vector (pREP1, lane 6), and multicopy plasmids carrying the *alp14*$^+$ (lane 7) or *dis1*$^+$ gene (lane 8) were spotted after serial dilution on rich plates containing 10 μg/ml TBZ and incubated at 26°C for 3 days. (**B**) Lethal 'cut' phenotypes in the presence of TBZ. DAPI staining of *alp14-1270* cells incubated for 6 h in the presence of 50 μg/ml TBZ at 26°C is shown. The bar indicates 10 μm. (**C**) Viability loss. The indicated strains were grown in rich medium at 26°C and TBZ (50 μg/ml) was added. After appropriate dilution, cells were plated on rich YES plates to examine colony forming ability. Viability was calculated by dividing the number of colonies by the number of cells per culture. While *dis1-203* cells (squares) did not lose viability, *alp14-1270* (circles), *mad2*-deleted (crosses) or *mad2alp14-1270* cells (triangles) did sharply, but with similar kinetics. (**D**) Decline of H1 kinase activity in *alp14-1270* in the presence of TBZ. (**E**) Quantification of H1 kinase activity from the data in (D) (wild-type, squares; *alp14-1270*, circles). (**F**) Securin destruction. Immunoblotting was performed in wild-type cells and *alp14* mutants (containing integrated *cut2*$^+$-HA) upon addition of TBZ. (**G**) Quantification of securin levels from the data in (F). (**H**) Separation of sister chromatids. Centromere-marked GFP was observed after 3 h upon TBZ addition in wild-type (left) and *alp14* mutants (right), which contain *cen-LacO* and *GFP-LacI-NLS*. (**I**) Toxicity of overproduced Mad2 in *alp14-1270* cells. *alp14-1270* mutants were transformed with a vector or plasmid in which *mad2*$^+$ is under the control of the thiamine-repressible *nmt1* promoter. Transformants were streaked on minimal plates in the presence (upper) or absence (lower) of thiamine and incubated for 4 days at 26°C.

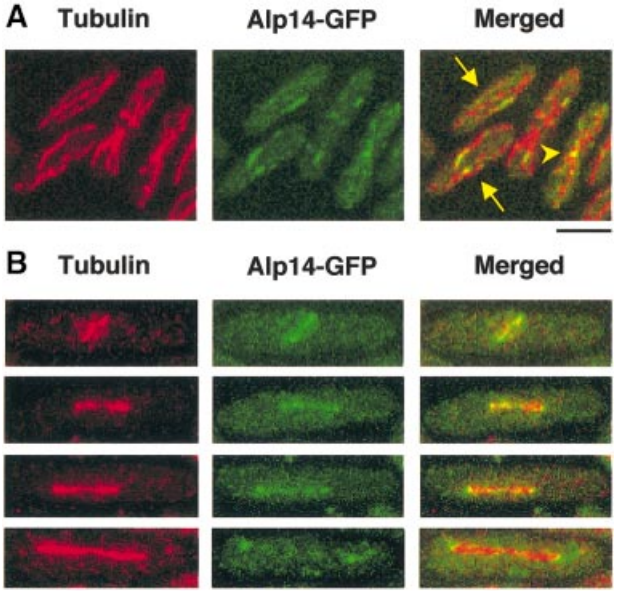

Fig. 5. Cellular localization of Alp14. Alp14 localization during the cell cycle. An integrated *alp14*$^{+}$*-GFP* strain was grown at 30°C, fixed with methanol (A) or formaldehyde (B) and processed for immunofluorescence microscopy. Anti-α-tubulin antibody (TAT-1) was used to visualize microtubules. A confocal microscope was used to observe each image. (**A**) Localization of Alp14 in interphase cells. Dotted staining along interphase microtubules (arrows) and localization at the equatorial ring in a post-anaphase cell (arrowhead) are shown. (**B**) Localization of Alp14 in mitotic cells. Phase 2 (top) or elongating anaphase cells (phase 3, lower three panels) are shown. The bar indicates 10 μm.

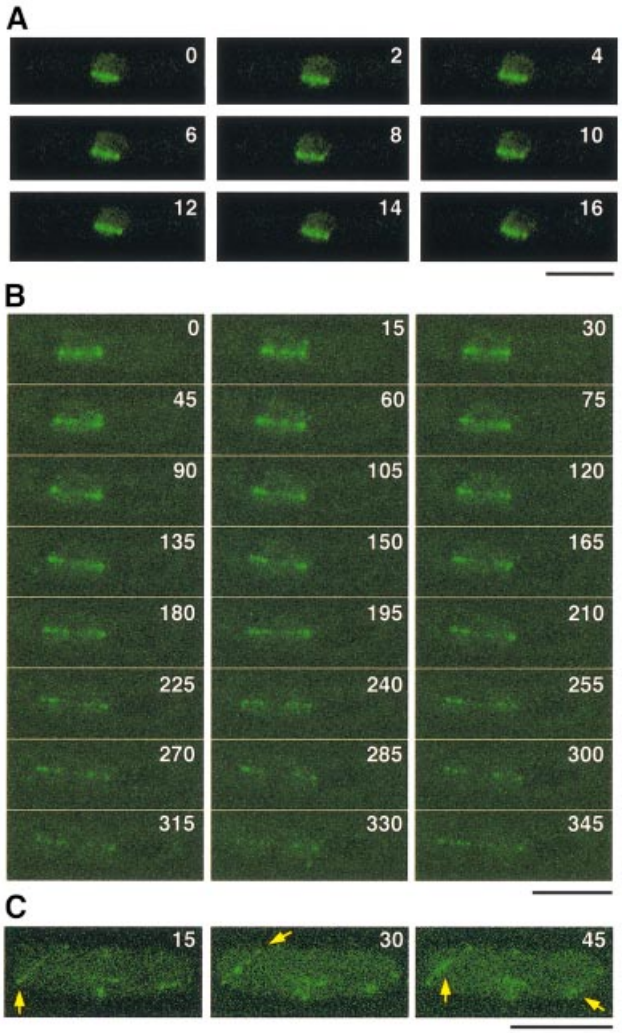

Fig. 6. Time-lapse imaging of Alp14–GFP during mitosis. (A–C) Live image analysis of Alp14–GFP. Time-lapse imaging of Alp14–GFP was performed using a conventional fluorescence microscope with 2 s intervals (**A**) or using confocal z-stack series, comprising 13 sections with a 0.36 μm step size with 15 s intervals (**B** and **C**). Mitotic cells of phase 2 (Nabeshima *et al.*, 1998) corresponding to prometaphase and metaphase are shown in (A). Spindles started to elongate in phase 3 of mitosis (at 75 s, in B). Post-anaphase cells are shown in (C). Alp14 co-localizing with astral microtubules is shown by arrows. See Supplementary data for live images. The bar indicates 10 μm.

seen in live images (see Figure 6A), and these dots may represent the kinetochores. In contrast, in *nda3* mutants, only a single dot instead of multiple dots was detected (Figure 7A, lower), which probably corresponded to the unseparated SPB (Ding *et al.*, 1997). This suggested that Alp14–GFP localization to the kinetochore periphery requires the mitotic spindle.

Next, co-localization between Alp14 and Mis6, a component of the fission yeast centromeres (Saitoh *et al.*, 1997), was addressed. To this end, ts *nuc2-663* cells containing doubly integrated *alp14*$^{+}$*-GFP* and *mis6*$^{+}$*-HA* were used. The dots of Alp14–GFP were visible along spindles, in addition to the two distal SPBs (visualized by anti-Sad1 antibodies; Hagan and Yanagida, 1995) (Figure 7B). Importantly, these inner dots overlapped, if not completely, with Mis6-HA. It is of note that the intranuclear dotted structures of Alp14–GFP appeared less defined in this image compared with the fixed samples shown before (Figure 7A) or non-fixed live images (see Figure 6A), which might be attributable to the procedures used for sample preparations for immunofluorescence microscopy.

The addition of TBZ to these *nuc2*-arrested cells resulted in the disappearance of Alp14–GFP dots (Figure 7C), providing further support that kinetochore localization of Alp14–GFP is dependent upon spindle integrity. On the other hand, SPB localization of Alp14–GFP and centromere localization of Mis6-HA were not disrupted by this treatment. Taken together, these results strongly suggest that Alp14 localizes to the kinetochore periphery at metaphase in a spindle-dependent fashion.

Alp14 is associated with the centromere DNA

Finally, to confirm the kinetochore localization of Alp14, the ChIP method (chromatin immunoprecipitation) (Hecht *et al.*, 1996; Ekwall *et al.*, 1997; Meluh and Koshland, 1997; Saitoh *et al.*, 1997; Ekwall and Partridge, 1999) was applied to *nuc2-663* mutants containing Alp14–GFP. Upon incubation at 36°C for 3 h, cells were fixed with formaldehyde and immunoprecipitation was performed with an anti-GFP antibody. A PCR then followed. The primers used were those encompassing the central region of the centromeres of chromosome I (*cnt1*) (Takahashi *et al.*, 1992; Saitoh *et al.*, 1997; Partridge *et al.*, 2000) and the flanking repeated region (*imr1* and *otr1*). As a control, a Mis6-Myc strain and primers for the non-centromeric region (*fbp1*) were also used. ChIP showed that Mis6 precipitated, as reported previously, with *cnt1* and *imr1*,

but not with *otr1* nor *fbp1* (Saitoh *et al*., 1997; Partridge *et al*., 2000). In *nuc2*-arrested cells, Alp14 precipitated with either *imr1* or *otr1* centromeric DNA (Figure 8A). We have failed so far to show any binding between Alp14 and *cnt1* DNA, the reasons for which might be technical in nature. Alternatively, Alp14 is indeed associated with the kinetochore periphery.

Next, ChIP was performed in the presence of TBZ in *nuc2-663* mutants (the same condition as in Figure 7C). Consistent with the dissociation of Alp14 from spindles and kinetochores, the binding of Alp14 to *imr1* or *otr1* was diminished (Figure 8A, four rightmost lanes). These results established that Alp14 is a mitosis-specific kinetochore-associated protein, the localization of which requires intact spindles.

Discussion

We have shown that the conserved Alp14 protein localizes to the kinetochore periphery and the poles during the mitotic stage and is a component of the Mad2-mediated spindle checkpoint (Figure 8B). We have also shown that the absence of Alp14 results in transient activation of this checkpoint pathway and this activation leads to mitotic delay in a Mad2-dependent fashion. Therefore, Alp14 apparently plays dual roles in this kinetochore-mediated pathway. One involves a regulatory function, in which Alp14 acts in a linear fashion with Mad2, probably upstream of it. The other role is structural, in which Alp14 is required for the interaction between the kinetochores and pole to chromosome microtubules. The dense short spindles seen at early mitosis in *alp14* mutants could be a result of either the inherent instability of pole to chromosome microtubules or the failure to capture the kinetochore, or in fact a combination of both. Mad2 localizes to these dots, which is consistent with the notion that these represent unattached kinetochores. In addition to activation of the Mad2-dependent spindle checkpoint, *alp14* mutants show Mad2-independent division delay. Although the molecular basis of this second block is currently elusive, it might be related to a post-anaphase delay; it is possible that the aberrant anaphase spindle assembled in the *alp14* mutant slows down the anaphase process and, as a result, leads to cell division delay.

Activation of the Mad2 checkpoint and loss of checkpoint activation in *alp14* mutants might seem to be a contradiction. However, it should be noted that the involvement of Alp14 in the Mad2-dependent checkpoint pathway becomes most evident under conditions when microtubules are depolymerized at the permissive temperature in *alp14* mutants, as the Mad2-dependent checkpoint pathway is dispensable for normally dividing cells in yeast. In contrast, the activation of the checkpoint in the *alp14* mutant is observed at high temperature, in which Alp14 is essential for cell division and required for the formation of functional pole to kinetochore spindles. These two phenotypes, therefore, would not be conflicting, but rather represent distinct aspects of Alp14 function. It is also of note that activation of the checkpoint in *alp14* mutants is transient (Figure 8B). In other words, in the absence of Alp14 function, the Mad2 checkpoint could sense the spindle damage, but the unattached kinetochores fail to maintain Mad2 localization and mitotic arrest.

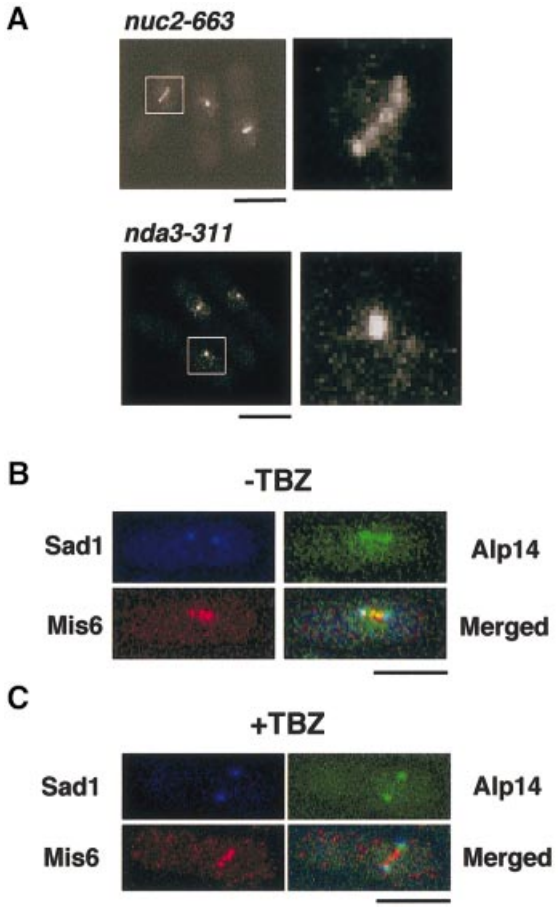

Fig. 7. Localization of Alp14 at the kinetochore periphery in metaphase. (**A**) Alp14 localization in *nuc2*- or *nda3*-arrested cells. *nuc2-663* (upper) or *nda3-311* (lower) cells containing integrated *alp14*$^{+}$*-GFP* are arrested at 36°C for 3 h or at 18°C for 8 h, respectively, fixed with formaldehyde and observed by confocal microscopy. Three individual cells are shown in each left panel and enlarged GFP images (6-fold) are shown on the right. The bar indicates 10 μm. (**B**) Localization of Alp14 and Mis6 in metaphase-arrested cells. *nuc2-663* cells containing integrated *alp14*$^{+}$*-GFP* and *mis6*$^{+}$*-HA* were arrested at 36°C for 3 h. Then cells were fixed, and signals from Alp14–GFP, anti-HA and anti-Sad1 antibodies were observed. (**C**) Dependence of kinetochore localization of Alp14 upon spindles. *nuc2-663* arrested cells in (B) were treated with TBZ (50 μg/ml) and, after 15 min, cells were processed for immunofluorescence microscopy. The bar indicates 10 μm.

Similar, if not identical, checkpoint-deficient phenotypes have been reported recently in other conserved components of the kinetochores (e.g. Spc24) and, interestingly, these proteins were identified originally as the components of the SPB (Wigge *et al*., 1998; Janke *et al*., 2001; Wigge and Kilmartin, 2001).

In spite of the evolutionary conservation of overall protein structure, kinetochore localization has not been reported before in other members of the TOG/XMAP215 proteins; instead, what is common is their localization to microtubules and the spindle poles (centrosomes) (Popov *et al*., 2001). This could simply be due to species-specific diversity between related proteins. Alternatively, the localization to the kinetochores may be too dynamic to be detected with conventional fluorescence microscopy of fixed samples. As shown in this study, only time-lapse live images using chromosomally integrated Alp14–GFP and

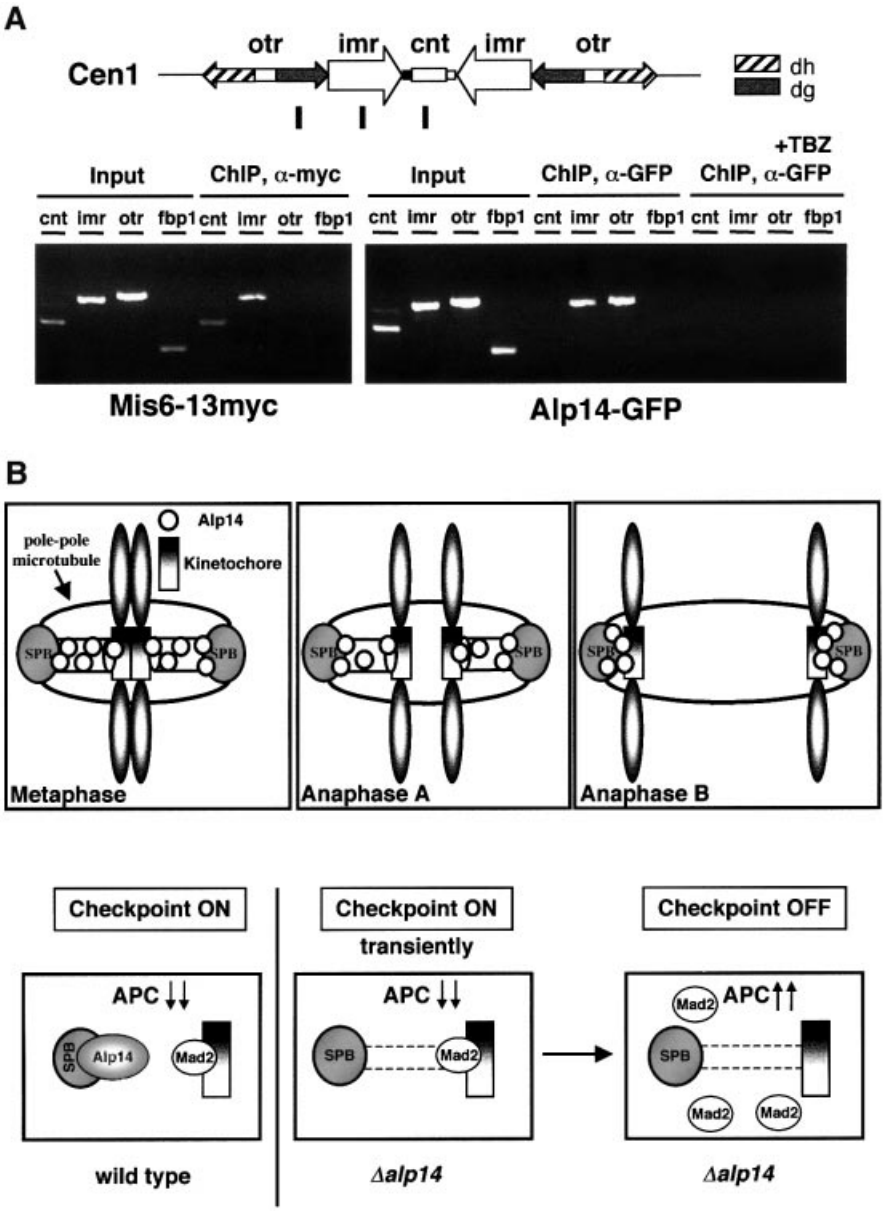

Fig. 8. Association of Alp14 with the centromere DNA and model for Alp14 function at kinetochores. (**A**) Association of Alp14 with the centromeric DNA. ChIP was performed in *nuc2-663* arrested cells containing integrated *alp14*$^{+}$*-GFP*. Cells were incubated at 36°C for 3 h and fixed with 1% formaldehyde. A schematic diagram showing the centromeric region of chromosome I is also shown. (**B**) A role for Alp14 in the kinetochores and the spindle checkpoint. Alp14 localizes to mitotic spindles, the SPBs and the kinetochore periphery during mitosis (upper). In the absence of Alp14, the spindle checkpoint failed to maintain the activation status, although Mad2 is capable of localizing to the kinetochores transiently. When microtubules and spindles are damaged or depolymerized, Alp14 is required for the activation of the Mad2-mediated spindle checkpoint.

also ChIP performed in metaphase-arrested cells have provided convincing data of kinetochore localization. Support for a role of Alp14 in kinetochore function comes from a number of previous reports (Gard and Kirschner, 1987; Vasquez *et al*., 1994; Tournebize *et al*., 2000), which pointed out the close involvement of XMAP215 in plus end-dependent microtubule dynamics, and, importantly, the plus end is where the kinetochore binds the mitotic spindle. We show that kinetochore localization of Alp14 is dependent upon the presence of intact spindles, which suggests that Alp14 passes through microtubules to attach to the kinetochores and its attachment would be transient. Whether or not all the TOG/XMAP215 family members attach to the kinetochores awaits careful localization studies in other organisms.

Although most of Alp14 dissociates from the kinetochores in the absence of intact spindles, it must execute a crucial role in activation of the checkpoint at the kinetochores. It should be pointed out that the SPB and the centromeres locate in close proximity under conditions of checkpoint activation (Funabiki *et al*., 1993). It is possible that Alp14 interacts directly or indirectly with checkpoint proteins and/or other regulators of kinetochore function. In dividing cells, Mad2 localization at the kinetochores appears to utilize microtubules and it travels between the kinetochores and the poles (Howell *et al*.,

Table II. Strain list

Strains	Genotypes	Derivations
HM123	*h⁻leu1*	our stock
DH1270	*h⁻leu1alp14-1270*	our stock
Δatb2	*h⁻leu1atb2::LEU2*	our stock
NC102	*h⁻leu1nuc2-663*	our stock
Δdis1	*h⁻leu1ura4dis1::ura4⁺*	Nabeshima *et al*. (1995)
AE148	*h⁻leu1ura4mad2::ura4⁺*	Kim *et al*. (1998)
HF178	*h⁺leu1cut2⁺-3HA-LEU2*	Funabiki *et al*. (1996)
GFP-nmt1-atb2	*h⁻leu1kan^r-nmt1-GFP-atb2⁺*	this study
GFP-nmt81-atb2	*h⁻leu1kan^r-nmt81-GFP-atb2⁺*	this study
HM248	*h⁻his2ade6-M210* containing Ch16 (mini-chromosome)	Niwa *et al*. (1989)
NK04	*h⁻leu1ura4 alp14::kan^r*	this study
MKY7A-4	*h⁺leu1ura4lys1his7LacO-lys1⁺GFP-LacI-NLS-his7⁺*	Nabeshima *et al*. (1995)
MAG000	*h⁻leu1ura4 alp14-1270mad2::ura4⁺*	this study
MAG004	*h⁻leu1ura4his7alp14⁺-GFP-kan^r*	this study
MAG031	*h⁻leu1nuc2-663alp14⁺-GFP-kan^r*	this study
MAG037	*h⁺leu1nda3-KM311alp14⁺-GFP-kan^r*	this study
MAG040	*h⁺leu1ura4his2alp14-1270 cut12⁺-GFPura4⁺*	this study
MAG050	*h⁻leu1alp14-1270LacO-lys1⁺GFP-LacI-NLS-his7⁺*	this study
MAG068	*h⁺leu1alp14-1270cut2⁺-3HA-LEU2*	this study
MAG071	*h⁻leu1ura4mad2⁺-GFP-kan^r*	this study
MAG074	*h⁻leu1ura4mis6⁺-13myc-kan^r*	this study
MAG090	*h⁻leu1ura4alp14-1270mad2⁺-GFP-kan^r*	this study
MAG092	*h⁻leu1nuc2-663alp14⁺-GFP-kan^rmis6⁺-3HA-kan^r*	this study
MAG117	*h⁻leu1nda3-311mad2⁺-GFP-kan^r*	this study

2000). Vertebrate CENP-E kinesin and yeast Spc24 play a role similar to Alp14 (Abrieu *et al*., 2000; Yao *et al*., 2000; Janke *et al*., 2001; Wigge and Kilmartin, 2001). It would be of interest to see whether TOG/XMAP215 interacts with these proteins. Although there are no obvious homologues to CENP-E in fission yeast, the dynamic behaviour of Alp14 on microtubules and spindles suggests the existence of motor molecules, which directly or indirectly interact with Alp14. Identification of such motor molecule(s) would be the next goal towards understanding the molecular anatomy of the kinetochore.

The kinetochore-mediated mitotic role of Alp14 is not its sole function. As *alp14* mutants show growth polarity defects (Radcliffe *et al*., 1998) and shorter interphase microtubules, we think that like XMAP215 (Gard and Kirschner, 1987; Vasquez *et al*., 1994), Alp14 also regulates the dynamics of cytoplasmic microtubules. The TOG/XMAP215-related proteins could be general plus end regulators of both interphase microtubules and mitotic spindles.

Materials and methods

Strains, media and genetic methods

Strains used in this study are listed in Table II. The standard methods were followed as described (Moreno *et al*., 1991).

Synchronous culture analysis

Small early G_2 cells were collected from exponentially growing cultures at 26°C by centrifugal elutriation, and were divided into two halves. One half continued to be incubated at 26°C to monitor the degree of synchrony, whilst the other half was shifted up to 36°C to observe defective phenotypes.

Cloning of the alp14⁺ gene

A *Schizosaccharomyces pombe* genomic library in a *LEU2*-based multicopy vector pAL-KS (obtained from Taro Nakamura) was used for the isolation of the *alp14⁺* gene. Seven transformants of an *alp14-1270* strain, which were Ts⁺ in a plasmid-dependent manner, were obtained from 10 000 Leu⁺ transformants. Plasmid DNAs were recovered from each transformant, and restriction mapping showed that all the plasmids contained an overlapping insert. Identification of the cloned gene as *alp14⁺* was confirmed by genetic crosses between tagged strains (*alp14⁺-GFP-kan^r*) and the original ts *alp14-1270* mutant.

Preparation and manipulation of nucleic acids

Enzymes were used as recommended by the suppliers (New England Biolabs). Nucleotide sequence data reported in this paper are in the DDBJ/EMBL/GenBank databases under the accession No. AB032409 (*alp14⁺*).

C-terminal epitope tagging

C-terminal tagging of Alp14 with GFP, Mis6 with 13Myc or 3HA, or Mad2 with GFP was performed by a PCR-based gene targeting method (Bähler *et al*., 1998).

Histone H1 kinase assay

H1 kinase assay was performed using $p13^{suc1}$ agarose beads (Oncogene) in the presence of [γ-^{32}P]ATP. Kinase activities were quantified by a Molecular Dynamics PhosphorImager.

Immunochemical assays

Affinity-purified rabbit polyclonal anti-Sad1 antibody was obtained from Dr Mizuki Shimanuki. Mouse monoclonal anti-α-tubulin antibody (TAT-1) was provided by Dr Keith Gull. Mouse monoclonal anti-Myc (9E10; BAbCO), anti-HA (16B12; BAbCO) and anti-GFP (Clones 7.1 and 13.1; Boehringer Mannheim) antibodies were also used.

Indirect immunofluorescence microscopy

Cells were fixed with methanol or formaldehyde, and primary antibodies (TAT-1 1:50, anti-Sad1 antibody 1:10 000 or anti-HA antibody 1:1000) were applied, followed by Cy3-conjugated goat anti-rabbit or anti-mouse IgG (Sigma), fluorescein-linked sheep anti-mouse IgG (Amersham) or Cy5-conjugated donkey anti-mouse IgG (Jackson Laboratories). Immunofluorescence images were viewed with a chilled video-rated CCD camera (model C5985; Hamamatsu) connected to a computer (Apple Power Macintosh G3/400) or with a laser scanning confocal microscope LSM510 (Zeiss Co.) and processed by use of Adobe® Photoshop (version 5.5).

Time-lapse live imaging

Rich medium containing 2% agar was solidified on a glass slide and one drop of the culture of a strain containing the chromosomal *alp14*$^{+}$*-GFP* was placed on top of the agar and sandwiched with a coverslip. Live images were taken at room temperature with a Zeiss Axioplan equipped with a chilled video CCD camera (C4742-95) and the PC computer containing kinetic image AQM software (Kinetic Imaging Ltd) or with a Zeiss LSM510 laser scanning confocal microscope under conditions as described previously (Brunner and Nurse, 2000). Z-stacks (200–400 nm steps) were taken every 15 s for maximally 12 min for a single preparation.

Formaldehyde cross-linked ChIP

The method previously described (Ekwall and Partridge, 1999) was followed with the following modifications: immunoprecipitates were washed sequentially with 1 ml of lysis buffer, 1 ml of lysis buffer containing 0.5 M NaCl and 1 ml of TE buffer. *nuc2-663* containing the chromosomal *alp14*$^{+}$*-GFP* or wild-type containing the chromosomal *mis6*$^{+}$*-13myc* was grown at 36°C for 3 h, fixed with 1% formaldehyde and soluble chromatin was prepared. Immunoprecipitations were performed with anti-GFP or anti-Myc antibody. Recovered DNA was assayed by PCR (35 cycles). Primer pairs used are as follows: 5′-AACAATAAACACGAATGCCTC-3′ plus 5′-ATAGTACCATGCGATTGTCTG-3′ for *cnt1*, 5′-GATGGAGAGTTACGAGGTAAAATG-3′ plus 5′-AATTGAATGAGAATCTGTGTACAG-3′ for *imr1*, 5′-CAACATTCGAAAATTCAAGGGAAA-3′ and 5′-CCGCAGCATATTGGTCGTCGTTTTTAA-3′ for *otr1*, and 5′-AATGACAATTCCCCACTAGCC-3′ plus 5′-ACTTCAGCTAGGATTCACCTGG-3′ for *fbp1*.

Supplementary data

Live images of Alp14–GFP can be seen as Supplementary data available at *The EMBO Journal* Online.

Acknowledgements

We thank Drs Iain M.Hagan, Tomohiro Matsumoto, Taro Nakamura, Yukinobu Nakaseko, Osami Niwa, Paul Nurse, Shelley Sazer, Mizuki Shimanuki, Chikashi Shimoda and Mitsuhiro Yanagida for providing materials used in this study, Satoko Yamaguchi and Hiroyuki Yamano for showing us the H1 kinase assay, Heidi Browning, Damian Brunner and Teresa Niccoli for instructions in live imaging, and Peter Jordan for help with confocal microscopy. Special thanks are given to Drs Robin C.Allshire and Janet F.Partridge for instruction in the ChIP method. We are grateful to Drs Anabelle Decottignies, Tatsuya Hirano, Tomohiro Matsumoto, Yukinobu Nakaseko and Hiroyuki Ohkura for informing us of unpublished results prior to publication, Kanji Furuya and Mitsuhiro Yanagida for information on Dis1 and Mad2 localization, Satoru Uzawa for stimulating discussion, Drs Jacqueline Hayles and Frank Uhlman for critical reading of the manuscript and useful suggestions, and the two anonymous referees, who helped improve this paper considerably. M.A.G. was supported by an EMBO long-term fellowship. This work is supported by the ICRF and the HFSP research grant.

References

Abrieu,A., Kahana,J.A., Wood,K.W. and Cleveland,D.W. (2000) CENP-E as an essential component of the mitotic checkpoint *in vitro*. *Cell*, **102**, 817–826.

Andrade,M.A. and Bork,P. (1995) HEAT repeats in the Huntington's disease protein. *Nature Genet.*, **11**, 115–116.

Bähler,J., Wu,J., Longtine,M.S., Shah,N.G., McKenzie,A.,III, Steever, A.B., Wach,A., Philippsen,P. and Pringle,J.R. (1998) Heterologous modules for efficient and versatile PCR-based gene targeting in *Schizosaccharomyces pombe*. *Yeast*, **14**, 943–951.

Bridge,A.J., Morphew,M., Bartlett,R. and Hagan,I.M. (1998) The fission yeast SPB component Cut12 links bipolar spindle formation to mitotic control. *Genes Dev.*, **12**, 927–942.

Brunner,D. and Nurse,P. (2000) CLIP170-like tip1p spatially organizes microtubular dynamics in fission yeast. *Cell*, **102**, 695–704.

Cahill,D.P., Lengauer,C., Yu,J., Riggins,G.J., Willson,J.K.V., Markowitz, S.D., Kinzler,K.W. and Vogelstein,B. (1998) Mutations of mitotic checkpoint genes in human cancers. *Nature*, **392**, 300–303.

Charrasse,S., Mazel,M., Taviaux,S., Berta,P., Chow,T. and Larroque,C. (1995) Characterization of the cDNA and pattern of expression of a new gene over-expressed in human hepatomas and colonic tumors. *Eur. J. Biochem.*, **234**, 406–413.

Charrasse,S., Schroeder,M., Gauthier-Rouviere,C., Ango,F., Cassimeris,L., Gard,D.L. and Larroque,C. (1998) The TOGp protein is a new human microtubule-associated protein homologous to the *Xenopus* XMAP215. *J. Cell Sci.*, **111**, 1371–1383.

Chen,R.-H., Waters,J.C., Salmon,E.D. and Murray,A.W. (1996) Association of spindle assembly checkpoint component XMAD2 with unattached kinetochores. *Science*, **274**, 242–246.

Chen,R.-H., Shevchenko,A., Mann,M. and Murray,A.W. (1998) Spindle checkpoint protein Xmad1 recruits Xmad2 to unattached kinetochores. *J. Cell Biol.*, **143**, 283–295.

Chen,X.P., Yin,H. and Huffaker,T.C. (1998) The yeast spindle pole body component Spc72p interacts with Stu2p and is required for proper microtubule assembly. *J. Cell Biol.*, **141**, 1169–1179.

Cullen,C.F., Deák,P., Glover,D.M. and Ohkura,H. (1999) *mini spindles*: a gene encoding a conserved microtubule-associated protein required for the integrity of the mitotic spindle in *Drosophila*. *J. Cell Biol.*, **146**, 1005–1018.

Ding,R., West,R.R., Morphew,M., Oakley,B.R. and McIntosh,J.R. (1997) The spindle pole body of *Schizosaccharomyces pombe* enters and leaves the nuclear envelope as the cell cycle proceeds. *Mol. Biol. Cell*, **8**, 1461–1479.

Ekwall,K. and Partridge,J.F. (1999) Fission yeast chromosome analysis: fluorescence *in situ* hybridisation (FISH) and chromatin immunoprecipitation (CHIP). In Bickmore,W.A. (ed.), *Chromosome Structural Analysis: A Practical Approach*. Oxford University Press, Oxford, UK, pp. 39–57.

Ekwall,K., Olsson,T., Turner,B.M., Cranston,G. and Allshire,R.C. (1997) Transient inhibition of histone deacetylation alters the structural and functional imprint at fission yeast centromeres. *Cell*, **91**, 1021–1032.

Funabiki,H., Hagan,I.M., Uzawa,S. and Yanagida,M. (1993) Cell cycle-dependent specific positioning and clustering of centromeres and telomeres in fission yeast. *J. Cell Biol.*, **121**, 961–976.

Funabiki,H., Yamano,H., Kumada,K., Nagao,K., Hunt,T. and Yanagida,M. (1996) Cut2 proteolysis required for sister-chromatid separation in fission yeast. *Nature*, **381**, 438–441.

Gard,D.L. and Kirschner,M.W. (1987) A microtubule-associated protein from *Xenopus* eggs that specifically promotes assembly at the plus-end. *J. Cell Biol.*, **105**, 2203–2215.

Groves,M.R., Hanlon,N., Turowski,P., Hemmings,B.A. and Barford,D. (1999) The structure of the protein phosphatase 2A PR65/A subunit reveals the conformation of its 15 tandemly repeated HEAT motifs. *Cell*, **96**, 99–110.

Hagan,I. and Yanagida,M. (1995) The product of the spindle formation gene *sad1*$^{+}$ associates with the fission yeast spindle pole body and is essential for viability. *J. Cell Biol.*, **129**, 1033–1047.

He,X., Patterson,T.E. and Sazer,S. (1997) The *Schizosaccharomyces pombe* spindle checkpoint protein mad2p blocks anaphase and genetically interacts with the anaphase-promoting complex. *Proc. Natl Acad. Sci. USA*, **94**, 7965–7970.

Hecht,A., Strahl-Bolsinger,S. and Grunstein,M. (1996) Spreading of transcriptional repressor SIR3 from telomeric heterochromatin. *Nature*, **383**, 92–96.

Hirano,T., Hiraoka,Y. and Yanagida,M. (1988) A temperature-sensitive mutation of the *S.pombe* gene *nuc2*$^{+}$ that encodes a nuclear scaffold-like protein blocks spindle elongation in mitotic anaphase. *J. Cell Biol.*, **106**, 1171–1183.

Hiraoka,Y., Toda,T. and Yanagida,M. (1984) The *NDA3* gene of fission yeast encodes β-tubulin: a cold-sensitive *nda3* mutation reversibly blocks spindle formation and chromosome movement in mitosis. *Cell*, **39**, 349–358.

Hirata,D., Masuda,H., Eddison,M. and Toda,T. (1998) Essential role of tubulin-folding cofactor D in microtubule assembly and its association with microtubules in fission yeast. *EMBO J.*, **17**, 658–666.

Howell,B.J., Hoffman,D.B., Fang,G., Murray,A.W. and Salmon,E.D. (2000) Visualization of Mad2 dynamics at kinetochores, along spindle fibers and at spindle poles in living cells. *J. Cell Biol.*, **150**, 1233–1250.

Hoyt,M.A., Totis,L. and Roberts,B.T. (1991) *S.cerevisiae* genes required for cell cycle arrest in response to loss of microtubule function. *Cell*, **66**, 507–117.

Hwang,L.H., Lau,L.F., Smith,D.L., Mistrot,C.A., Hardwick,K.G., Hwang,E.S., Amon,A. and Murray,A.W. (1998) Budding yeast Cdc20: a target of the spindle checkpoint. *Science*, **279**, 1041–1044.

Janke,C., Ortiz,J., Lechner,J., Shevchenko,A., Shevchenko,A., Magiera,

M.M., Schramm,C. and Schiebel,E. (2001) The budding yeast proteins Spc24p and Spc25p interact with Ndc80p and Nuf2p at the kinetochore and are important for kinetochore clustering and checkpoint control. *EMBO J.*, **20**, 777–791.

Jin,D.-Y., Spencer,F. and Jeang,K.-T. (1998) Human T cell leukemia virus type 1 oncoprotein tax targets the human mitotic checkpoint protein MAD1. *Cell*, **93**, 81–91.

Kim,S.H., Lin,D.P., Matsumoto,S., Kitazono,A. and Matsumoto,T. (1998) Fission yeast Slp1: an effector of the Mad2-dependent spindle checkpoint. *Science*, **279**, 1045–1047.

King,R.W., Peters,J.-M., Tugendreich,S.T., Rolfe,M., Hieter,P. and Kirschner,M.W. (1995) A 20S complex containing CDC27 and CDC16 catalyzes the mitotic-specific conjugation of ubiquitin to cyclin B. *Cell*, **81**, 279–288.

King,R.W., Deshaies,R.J., Peters,J.-M. and Kirschner,M.W. (1996) How proteolysis drives the cell cycle. *Science*, **274**, 1652–1659.

Lengauer,C., Kinzler,K.W. and Vogelstein,B. (1998) Genetic instabilities in human cancers. *Nature*, **396**, 643–649.

Li,R. and Murray,A.W. (1991) Feedback control of mitosis in budding yeast. *Cell*, **66**, 519–531.

Li,Y. and Benezra,R. (1996) Identification of a human mitotic checkpoint gene: *hsMAD2*. *Science*, **274**, 246–248.

Matthews,L.R., Carter,P., Thierry-Mieg,D. and Kemphues,K. (1998) ZYG-9, a *Caenorhabditis elegans* protein required for microtubule organization and function, is a component of meiotic and mitotic spindle poles. *J. Cell Biol.*, **141**, 1159–1168.

Meluh,P.B. and Koshland,D. (1997) Budding yeast centromere composition and assembly as revealed by *in vivo* cross-linking. *Genes Dev.*, **11**, 3401–3412.

Moreno,S., Klar,A. and Nurse,P. (1991) Molecular genetic analyses of fission yeast *Schizosaccharomyces pombe*. *Methods Enzymol.*, **194**, 795–823.

Nabeshima,K., Kurooka,H., Takeuchi,M., Kinoshita,K., Nakaseko,Y. and Yanagida,M. (1995) p93dis1, which is required for sister chromatid separation, is a novel microtubule and spindle pole body-associating protein phosphorylated at the Cdc2 target sites. *Genes Dev.*, **9**, 1572–1585.

Nabeshima,K., Nakagawa,T., Straight,A.F., Murray,A., Chikashige,Y., Yamashita,Y.M., Hiraoka,Y. and Yanagida,M. (1998) Dynamics of centromeres during metaphase–anaphase transition in fission yeast: Dis1 is implicated in force balance in metaphase bipolar spindle. *Mol. Biol. Cell*, **9**, 3211–3225.

Nakaseko,Y., Nabeshima,K., Kinoshita,K. and Yanagida,M. (1996) Dissection of fission yeast microtubule associating protein p93dis1: regions implicated in regulated localization and microtubule interaction. *Genes Cells*, **1**, 633–644.

Neuwald,A.F. and Hirano,T. (2000) HEAT repeats associated with condensins, cohesins and other complexes involved in chromosome-related functions. *Genome Res.*, **10**, 1445–1452.

Niwa,O., Matsumoto,T., Chikashige,Y. and Yanagida,M. (1989) Characterization of *Schizosaccharomyces pombe* minichromosome deletion derivatives and a functional allocation of their centromere. *EMBO J.*, **8**, 3045–3052.

Ohkura,H., Adachi,Y., Kinoshita,N., Niwa,O., Toda,T. and Yanagida,M. (1988) Cold-sensitive and caffeine supersensitive mutants of the *Schizosaccharomyces pombe dis* genes implicated in sister chromatid separation during mitosis. *EMBO J.*, **7**, 1465–1473.

Partridge,J.F., Borgstrøm,B. and Allshire,R.C. (2000) Distinct protein interaction domains and protein spreading in a complex centromere. *Genes Dev.*, **14**, 783–791.

Popov,A.V., Pozniakovsky,A., Arnal,I., Antony,C., Ashford,A., Kinoshita,K., Tournebize,R., Hyman,A.A. and Karsenti,E. (2001) XMAP215 regulates microtubule dynamics through two distinct domains. *EMBO J.*, **20**, 397–410.

Radcliffe,P., Hirata,D., Childs,D., Vardy,L. and Toda,T. (1998) Identification of novel temperature-sensitive lethal alleles in essential β-tubulin and nonessential α2-tubulin genes as fission yeast polarity mutants. *Mol. Biol. Cell*, **9**, 1757–1771.

Radcliffe,P.A., Hirata,D., Vardy,L. and Toda,T. (1999) Functional dissection and hierarchy of tubulin-folding cofactor homologues in fission yeast. *Mol. Biol. Cell*, **10**, 2987–3001.

Saitoh,S., Takahashi,K. and Yanagida,M. (1997) Mis6, a fission yeast inner centromere protein, acts during G_1/S and forms specialized chromatin required for equal segregation. *Cell*, **90**, 131–143.

Straight,A.F., Belmont,A.S., Robinett,C.C. and Murray,A.W. (1996) GFP tagging of budding yeast chromosomes reveals that protein–protein interactions can mediate sister chromatid cohesion. *Curr. Biol.*, **6**, 1599–1608.

Sudakin,V., Ganoth,D., Dahan,A., Heller,H., Hershko,J., Luca,F.C., Ruderman,J.V. and Hershko,A. (1995) The cyclosome, a large complex containing cyclin-selective ubiquitin ligase activity, targets cyclins for destruction at the end of mitosis. *Mol. Biol. Cell*, **6**, 185–198.

Takahashi,K., Murakami,S., Chikashige,Y., Funabiki,H., Niwa,O. and Yanagida,M. (1992) A low copy number central sequence with strict symmetry and unusual chromatin structure in fission yeast centromere. *Mol. Biol. Cell*, **3**, 819–835.

Taylor,S.S. and McKeon,F. (1997) Kinetochore localization of murine Bub1 is required for normal mitotic timing and checkpoint response to spindle damage. *Cell*, **89**, 727–735.

Taylor,S.S., Ha,E. and McKeon,F. (1998) The human homologue of Bub3 is required for kinetochore localization of Bub1 and a Mad3/Bub1-related protein kinase. *J. Cell Biol.*, **142**, 1–11.

Tournebize,R. *et al*. (2000) Control of microtubule dynamics by the antagonistic activities of XMAP215 and XKCM1 in *Xenopus* egg extracts. *Nature Cell Biol.*, **2**, 13–19.

Vardy,L. and Toda,T. (2000) The fission yeast γ-tubulin complex is required in G_1 phase and is a component of the spindle-assembly checkpoint. *EMBO J.*, **19**, 6098–6111.

Vasquez,R.J., Gard,D.L. and Cassimeris,L. (1994) XMAP from *Xenopus* eggs promotes rapid plus end assembly of microtubules and rapid microtubule polymer turnover. *J. Cell Biol.*, **127**, 985–993.

Wang,P.J. and Huffaker,T.C. (1997) Stu2p: a microtubule-binding protein that is an essential component of the yeast spindle pole body. *J. Cell Biol.*, **139**, 1271–1280.

Waters,J.C., Chen,R.-H., Murray,A.W. and Salmon,E.D. (1998) Localization of Mad2 to kinetochores depends on microtubule attachment, not tension. *J. Cell Biol.*, **141**, 1181–1191.

Weiss,E. and Winey,M. (1996) The *Saccharomyces cerevisiae* spindle pole body duplication gene *MPS1* is part of a mitotic checkpoint. *J. Cell Biol.*, **132**, 111–123.

Wigge,P.A. and Kilmartin,J.V. (2001) The Ndc80p complex from *Saccharomyces cerevisiae* contains conserved centromere components and has a function in chromosome segregation. *J. Cell Biol.*, **152**, 349–360.

Wigge,P.A., Jensen,O.N., Holmes,S., Souès,S., Mann,M. and Kilmartin,J.V. (1998) Analysis of the *Saccharomyces* spindle pole by matrix-assisted laser desorption/ionization (MALDI) mass spectrometry. *J. Cell Biol.*, **141**, 967–977.

Yao,X., Abrieu,A., Zheng,Y., Sullivan,K.F. and Cleveland,D.W. (2000) CENP-E forms a link between attachment of spindle microtubules to kinetochores and the mitotic checkpoint. *Nature Cell Biol.*, **2**, 484–491.

Received March 5, 2001; revised May 8, 2001; accepted May 9, 2001

Note added in proof

While this paper was under review, two papers appeared related to this work. One paper [Nakaseko,Y., Goshima,G., Morishita,J. and Yanagida,M. (2001) M phase-specific kinetochore proteins in fission yeast: microtubule-associated Dis1 and Mtc1 display rapid separation and segregation during anaphase. *Curr. Biol.*, **11**, 537–549] shows kinetochore localization of Dis1, whilst the other paper [Severin,F., Habermann,B., Huffaker,T. and Hyman,T. (2001) Stu2 promotes mitotic spindle elongation in anaphase. *J. Cell Biol.*, **153**, 435–442] shows activation of the spindle checkpoint in budding yeast ts *stu2* mutants.